Chemistry
A European
Journal

Chemistry
Europe
European Chemical
Societies Publishing

Accepted Article

Title: A Light-Harvesting/Charge-Separation Model with Energy Gradient Made of Assemblies of meta-pyridyl Zinc Porphyrins

Authors: Joe Otsuki, Takumi Okumura, Kosuke Sugawa, Shin-ichiro Kawano, Kentaro Tanaka, Takehiro Hirao, Takeharu Haino, Yu Jin Lee, Seongsoo Kang, and Dongho Kim

To be cited as: *Chem. Eur. J.* 10.1002/chem.202003327

Link to VoR: https://doi.org/10.1002/chem.202003327

WILEY-VCH

A Light-Harvesting/Charge-Separation Model with Energy Gradient Made of Assemblies of *meta*-Pyridyl Zinc Porphyrins

Joe Otsuki,*[a] Takumi Okumura,[a] Kosuke Sugawa,[a] Shin-ichiro Kawano,[b] Kentaro Tanaka,[b] Takehiro Hirao,[c] Takeharu Haino,[c] Yu Jin Lee,[d] Seongsoo Kang,[d] and Dongho Kim[d]

[a] Professor J. Otsuki, T. Okumura, and Dr. K. Sugawa
Department of Materials and Applied Chemistry, College of Science and Technology, Nihon University
1-8-14 Kanda Surugadai, Chiyoda-ku, Tokyo 101-8308 Japan
otsuki.joe@nihon-u.ac.jp
[b] Dr. S. Kawano and Prof. K. Tanaka
Department of Chemistry, Graduate School of Science, Nagoya University
Furocho, Chikusa-ku, Nagoya 464-8602, Japan
[c] Dr. T. Hirao and Professor T. Haino
Department of Chemistry, Graduate School of Advanced Science and Engineering, Hiroshima University
1-3-1 Kagamiyama, Higashi-Hiroshima, 739-8526 Japan
[d] Y. J. Lee, S. Kang, and Prof. D. Kim
Spectroscopy Laboratory for Functional π-Electronic Systems and Department of Chemistry, Yonsei University, Seoul 03722, South Korea

Supporting information for this article is given via a link at the end of the document.

Abstract: Self-assembly of porphyrins is a fascinating topic not only for mimicking chlorophyll assemblies in photosynthetic organisms but also for the potential of creating molecular-level devices. Herein we have prepared zinc porphyrin derivatives bearing a *meta*-pyridyl group at the *meso*-position and studied their assemblies in chloroform. Among porphyrins studied, one with a carbamoylpyridyl moiety (ZnPPyC) gave distinct ^{1}H NMR spectrum in $CDCl_3$, which allowed us to probe the supramolecular structure in solution in detail. Ring-current induced chemical shift changes in ^{1}H NMR, together with vapor pressure osmometry and diffusion-ordered NMR spectroscopy, among other evidence, suggested that the porphyrin molecules form a trimer in a triangular cone structure. Further incorporation of a directly-linked porphyrin-ferrocene dyads with the same assembling properties in the assemblies lead to a rare light-harvesting/charge-separation model, in which an energy gradient is incorporated and reductive quenching occurs.

Introduction

Porphyrins have been attracting interest of many researchers for a long time as archetypal photo/electro-active compounds [1]. Their unique photophysical properties are being explored as sensitizers in light-harvesting and charge separation model studies[2-5] as well as for solar cells[6-10] and medical applications,[11] among others.[12-14] Organizing porphyrin molecules is an important subject to take best advantage of capabilities of porphyrins.[5, 15-17]

Axial coordination of nitrogen containing heterocycles such as pyridine to zinc ion in the center of porphyrin macrocycle is one the simplest interactions that can be used for assembling porphyrins. Zinc complexes of porphyrin having pyridyl moieties assemble themselves into supramolecular species by mutual coordination. A particularly simple case is the self-assembly of zinc *meso*-(*para*-pyridyl)porphyrin, in which only one *meso*-position is substituted by the *para*-pyridyl group. In nonpolar solutions, four of these molecules self-assemble into a square by mutual axial coordination.[18-22] Zinc *meso*-(*para*-pyridylethynyl)porphyrin also forms a square in solution.[23] Interestingly, the same molecules form linear polymer-like coordination chains in the solid state as revealed by a crystal structure.[24] Formation of supramolecular square using a *para*-pyridyl unit was also applied to chlorophyll derivatives to prepare square-shaped chlorophyll assemblies.[25-28]

Much less is known for the assembling behavior of zinc *meso*-(*meta*-pyridyl)porphyrins. Aida et al. investigated assemblies of porphyrins with a *meta*-pyridyl substituent at one of the *meso* positions.[29] A crystal structure of a tetrameric assembly of one of the zinc *meta*-pyridiylporphyrins was reported but the information on the structures in solutions are not available except absorption spectra and mass spectra showing *m*/*z* signals up to the tetramer. A chlorophyll derivative bearing a *meta*-pyridyl group bridged by a phenylene ethynylene at the 20 position was reported to form a trimer.[30]

We have investigated the assembling behavior of some new zinc *meso*-(*meta*-pyridyl)porphyrins in chloroform solutions. The investigated porphyrins, which are shown in Scheme 1, include those bearing *meta*-pyridyl (ZnPPy), a *meta*-(3-acetamidopyridyl) (ZnPPyA), and *meta*-(3-carbamoylpyridyl) (ZnPPyC) substituents at the *meso*-position. We found that the carbamoylpyridyl derivative, among these porphyrin derivatives, gave well-resolved ^{1}H NMR spectra, which allowed us to investigate the structure of the assemblies in solution in detail. Furthermore, a light-harvesting and charge separation model was constructed by introducing a zinc carbamoylpyridylporphyrin bearing a ferrocene moiety into the assemblies. This is a rare example of supramolecular porphyrin-based light-harvesting/charge separation systems in which reductive quenching is involved.

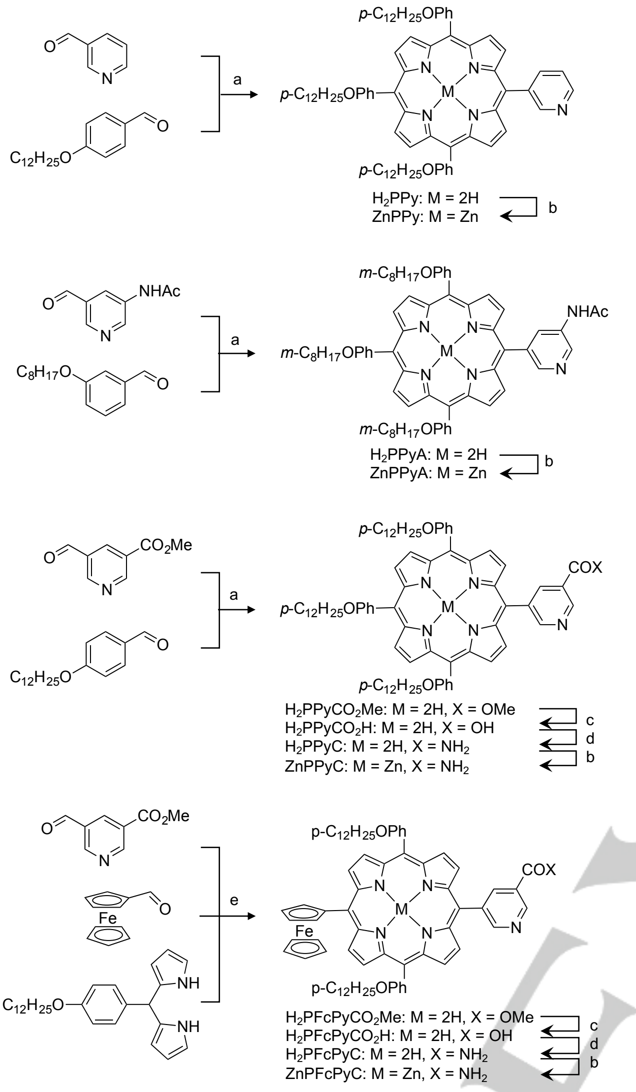

Scheme 1. Preparation of zinc *meso*-(*meta*-pyridyl)porphyrins derivatives. Reagents and conditions: a) pyrrole, propionic acid, reflux (H_2PPy: 3.3%; H_2PPyA: 13%; H_2PPyCO$_2$Me: 7.9%); b) Zn(OAc)$_2$ or Zn(OAc)$_2$•(H_2O)$_2$, $CHCl_3$, MeOH, rt (ZnPPy: 74%; ZnPPyA: 100%; ZnPPyC: 88%; ZnPFcPyC: 95%); c) (i) KOH, THF, H_2O, reflux, (ii) aq HCl (H_2PPyCO$_2$H: 71%; H_2PFcPyCO$_2$H: 93%); d) (i) CDI, THF, reflux, (ii) aq NH_3 (H_2PPyC: 71%; H_2PFcPyC: 98%); e) (1) TFA, NH_4Cl, CH_2Cl_2, rt, (ii) DDQ, (ii) Et_3N (H_2PFcPyCO$_2$Me: 3.0%).

Results and Discussion

Design and Synthesis

The motivation of using acetamido (in ZnPPyA) and carbamoyl (in ZnPPyC) moieties at the 3-position of the pyridyl group was to see if axial coordination and hydrogen bonding work synergistically in the binding of these molecules. The intermolecular hydrogen bonding with simultaneous coordination interaction would result in assemblies in which neighboring porphyrin macrocycles make a shallow angle as shown on the right in Figure 1. Repetition of these interactions would result in a large assembly in the form of a ring,[31] which is reminiscent of the light-harvesting antenna found in purple bacteria.[32-34] We found that, as discussed below, the structural information could be obtained for the carbamoylpyridyl derivative owing to its well-resolved ^{1}H NMR signals. The structure in solution turned out to be of the motif shown on the left in Figure 1.

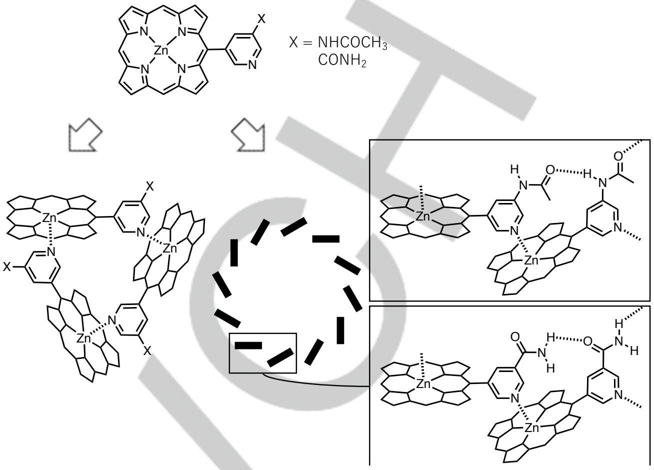

Figure 1. Possible motifs of assembly.

Scheme 1 displays the synthesis of *meso*-(*meta*-pyridyl)porphyrins which were investigated in the present study. Alkoxy chains were introduced to confer enough solubility to the porphyrins. These alkoxy chains were considered not to pose any steric problem in either type of the assemblies shown in Figure 1. The alkoxybendaldehyde derivatives were prepared from the corresponding hydroxybenzaldehyde precursors and bromoalkane in DMF in the presence of K_2CO_3.

The A_3B-type porphyrins were prepared by the classical Adler-Longo protocol[35] by feeding alkoxybenzaldehyde, pyridinecarboxaldehyde, and pyrrole in a ratio of 3:1:4. The desired A_3B-type porphyrin was eluted as a second band in silica gel chromatography following *meso*-tetra(alkoxyphenyl)porphyrin and was isolated in 3–13% yields. For the preparation of ZnPyC, methyl 5-formyl-3-pyridinecarboxylate was used in the porphyrin formation reaction. The methyl ester was hydrolyzed by KOH/THF/H_2O into the free carboxylic acid,[36-37] which was then transformed into the amide by treating with excess carbonyldiimidazole (CDI) followed by addition of aqueous ammonia.[38] Finally, zinc was inserted into the porphyrin by mixing the free-base porphyrin and Zn(OAc)$_2$ at room temperature.[39]

In the case of ZnPFcPyC, which is an A_2BC-type porphyrin, we chose the condensation of *meso*-(4-dodexyloxyphen-1-yl)-2,2'-dipyrromethane with 5-formyl-3-pyridinecarboxylate and ferrocenecarboxaldehyde using TFA as an acid catalyst and NH_4Cl as a water scavenger in CH_2Cl_2, followed by oxidation by DDQ.[40-41] Our concern was the scrambling of *meso*-substituents during the macrocyclization. Particularly, it was inferred that the electron-rich *meso*-substituent, *i.e.*, ferrocene, had detrimental effects promoting scrambling. Indeed, *meso*-tris(dodecyloxyphenyl)-(methoxycarbonylpyridyl)porphyrin, *i.e.*, H_2PPyCO$_2$Me, was contained in the products, which was a clear indication that scrambling took place. This byproduct, behaved similarly to the desired H_2PFcPyCO$_2$Me on the SiO_2 TLC and was difficult to be removed by SiO_2 chromatography. We could either purify the product by GPC at this stage or proceed to the following reactions with the mixture. In the latter case, the desired compound was purified by GPC at the stage of H_2PFcPyC. These porphyrins generally gave clean, nice signals corresponding to M^+ or MH^+ without appreciable fragmentation in the laser desorption ionization mass spectrometry without using any matrix (for MS spectra, see supporting information). We found, however, that signals are much smaller for ferrocene-containing porphyrins under similar ionization conditions.

Assembly Formation

The ^{1}H NMR spectrum for ZnPPy in $CDCl_3$ was untractably broad (See Figure S1a). Modification of the pyridyl group by 3-acetamido moiety (ZnPPyA) did not improve the situation (Figure S1b). These broadening is most likely caused by formation of some assemblies in solution. Indeed, the diffusion-ordered NMR spectroscopy (DOSY) measurements[42-44] for solutions in $CDCl_3$ (21 mM, 24 °C) gave values of diffusion constants (D) of 4.96 x 10^{-10} m^2 s^{-1} and 2.77 x 10^{-10} m^2 s^{-1} for H_2PPyA and ZnPPyA, respectively (Figure S2). These values of diffusion coefficients translate into hydrodynamic radiuses of 0.83 nm and 1.49 nm, respectively, according to the Stokes-Einstein formula:

$$r = \frac{k_B T}{6\pi\eta D} \quad (1)$$

in which k_B, T, and η (5.28 x 10^{-4} kg m^{-1} s^{-1} for $CDCl_3$[45]) are the Boltzmann constant, temperature, and the viscosity, respectively. The former value of 0.83 nm for the free-base porphyrin is consistent with the size of porphyrin molecule excluding the alkoxy chains; the H–H distance between the *para*-hydrogens of the phenyl moieties trans to each other of *meso*-tetraphenylporphyrin is 1.80 nm.[46] The radius for the zinc porphyrin counterpart is 1.8 times larger than that for the free-base porphyrin, which indicates the formation of some distinct, *i.e.*, not polymeric, supramolecular assembly. It was difficult to obtain further insight into the supramolecular structure in solution, however, because of the broad nature of the ^{1}H NMR spectrum.

Gratifyingly, modification of the pyridyl group by the 3-carbamoyl moiety sharpened up the peaks in the ^{1}H NMR spectrum, which allowed us to shed light on the structure of the supramolecular assembly in solution. The ^{1}H NMR spectrum for ZnPPyC is displayed in Figure 2 together with the spectrum for the free-base counterpart, H_2PPyC. Zinc insertion is indicated by the disappearance of the imine H signal observed at –2.76 ppm for the free-base porphyrin. The signals for the free-base porphyrin are symmetrical with respect to the pseudo-mirror plane passing through the porphine–pyridyl bond as expected. Also, there is no distinction between the two *ortho*-protons and two *meta*-protons of the phenyl groups. The number of protons assigned to each signal is, therefore, a multiple of two except for protons of the pyridyl group. On the other hand, this symmetry is lost in the zinc porphyrin, which suggests that some intermolecular association occurs leading to a structure with a lower symmetry and hindered rotation of *meso*-substituents. Partial assignment of signals for the zinc porphyrin was possible taking advantage of substantially different *J*-coupling constants depending on the fragment the protons belong to. The *J*-coupling constants between porphine protons, phenyl protons, and pyridyl protons are approximately ~5 Hz, ~8 Hz, and ~2 Hz. The fragments to which protons belong to are indicated on the peaks in Figure 2b, as judged by the coupling constants which are corroborated by the COSY spectrum (Figure S3). Particularly, the relatively small long-range coupling among pyridyl protons, $^4J_{H\text{-}H}$ was found by inserting a delay time of 50 ms in the COSY spectrum (long-range COSY). The pyridyl protons are located at 2.11, 3.37, and 6.68 ppm. These peaks are significantly shifted upfield compared to those of the free-base porphyrin, for which all three pyridyl protons are observed at >8.9 ppm. These large upfield shifts indicate that the pyridyl moiety coordinates axially to the zinc ion in the porphyrin macrocycle of another molecule.[47] It is likely that the 2.11 and 3.37 ppm peaks with particularly large upfield shifts are of protons *ortho* to the nitrogen. It is well known that pyridine commonly coordinates to the zinc ion in porphyrin in a perpendicular orientation.[48-49] The chemical shifts of the two ortho-protons are expected to be quite similar if this was the case. However, it is noteworthy that the chemical shift values for the ortho protons in the present case differ more than 1 ppm, which suggests that the environment around the coordination center is rather unsymmetrical.

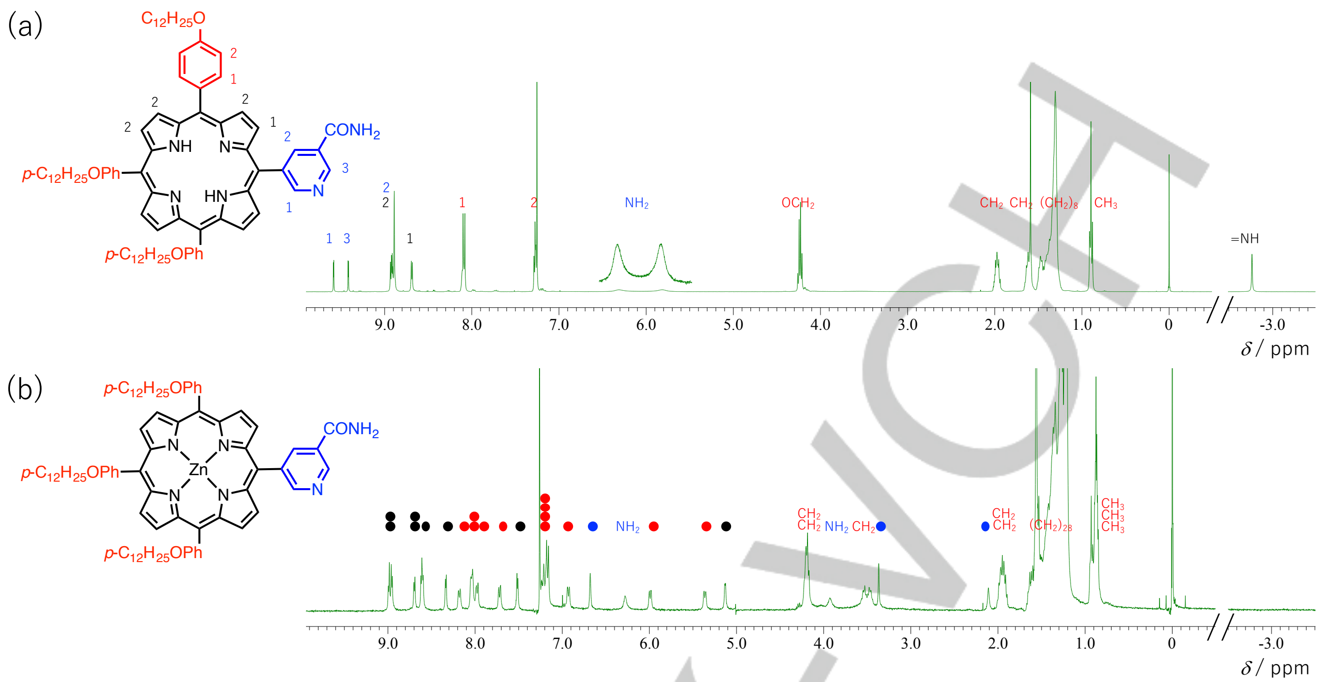

Figure 2. ^{1}H NMR spectra in $CDCl_3$. The colors represent the fragment to which a proton belongs (black: porphine, blue: pyridyl, red: dodecyloxyphenyl). (a) H_2PPyC. (b) ZnPPyC. Each of the dots represents a proton.

To get insight into the stability and possible dynamic nature of the assembly, ^{1}H NMR spectra for a 5 mM sample in $CDCl_3$ were taken in a wide range of temperatures from –50 °C to 50 °C. Remarkably, there was almost no change in the spectra in this wide temperature range, except for a little broadening at the lowest and highest temperatures as shown in Figure S4. This observation strongly suggests that the assembly comprises a single species in solution, in which all molecules in the assembly are equivalent in the NMR time scale. Otherwise, equilibrium would shift from one to another if more than one species were involved. The equivalence of constituent molecules imply that the supramolecular assembly has a C_3 symmetry *on average*. This does not necessarily mean that the C_3 symmetrical structure is the most stable and the assembly stays in that structure but rather the assembly can fluctuate about the C_3 structure.

The observation that the spectra shows little changes over the wide range of temperature also indicates that the assembly is very stable. This in turn implies that the assembly is a *closed* structure. If the assembly consisted of an *open* structure, such as a linear assembly, the number of associated molecules in the assembly would be changed upon temperature variation. The stability was also shown by ^{1}H NMR spectra for diluted samples. There was practically no change in the spectra down to 0.1 mM from the spectrum at 5 mM, as shown in Figure S5. At a concentration as low as 0.02 mM, the spectrum showed a new pattern.

Absorption spectra corroborate that the axially coordinated species dominate at 0.1 mM. The spectra for ZnPPyC in chloroform in the Q-band region exhibits blue-shifts from a set of 566 nm and 610 nm to a set of 552 nm and 592 nm, respectively, upon dilution from 0.1 mM to 0.01 mM as shown in Figure S6. As the Q-band peaks for zinc *meso*-tetraphenylporphyrin appear at 550 nm and 593 nm, which are red-shifted by pyridine coordination by about 15 nm, the spectrum for the 0.1 mM sample represents the axially coordinated zinc porphyrin, while the spectrum for the 0.01 mM sample represents the dissociated free zinc porphyrin, and the intermediate spectra indicate the transition of equilibrium. The association constants for axial coordination of pyridyl ligands and zinc porphyrins are typically on the order of a few thousands M^{-1} in chloroform,[50] and hence the major equilibrium transition of coordinated species to dissociated species is expected to occur at around 1 mM. That this occurs at less than 0.1 mM in the present case suggests the involvement of some synergistic effect of intermolecular interactions, such as cyclic ring formation.[20]

Size of the assembly.

DOSY experiments were conducted for H_2PPyC and ZnPPyC to assess the size of the assembly in $CDCl_3$ (Figure S7). The diffusion coefficients obtained for H_2PPyC and ZnPPyC are 4.3 x 10^{-10} m^2 s^{-1} and 2.2 x 10^{-10} m^2 s^{-1}, respectively. These values translate into hydrodynamic radiuses of 0.96 nm and 1.88 nm, respectively. The former value is again consistent with the monomeric porphyrin, while the latter is twice as large.

The molecular weight information for the species in chloroform solution was obtained by the vapor pressure osmometry, as shown in Figure S8. The molecular weight of H_2PPy, which is incapable of coordination or hydrogen bonding, was obtained as 1312±48, which is close to the formula value of 1169. On the other hand, the molecular weight for ZnPPyC was obtained as 4260±220, which is 3.3 times as large as the formula value of 1275, suggesting that the assembly is a trimer.

Further Confirmation of Trimer Formation — Quenching Experiments

To confirm the trimer formation, we performed a quenching experiment using ZnPFcPyC. The idea behind this experiment was based on three assumptions as follows. (1) As this molecule is similar in shape to ZnPPyC and has the same components essential for the self-assembly as ZnPPyC, *i.e.*, the zinc ion and carbamolypyridyl moiety, this molecule would assemble in the same motif as ZnPPyC. This assertion was consistent with its ^{1}H NMR spectrum in $CDCl_3$, which is shown in Supporting Information. The spectrum indicated the loss of symmetry, which appears to be similar to the case for ZnPPyC, although, unfortunately, the peaks were not sharp enough to allow their assignments. When ZnPPyC and ZnPFcPyC are mixed, they would form statistically mixed assemblies. (2) The ferrocene unit of ZnPFcPyC would quench the singlet excited state of porphyrin, which renders the molecule nonfluorescent via reductive electron transfer, which was confirmed for directly-linked porphyrin-ferrocene conjugates[40, 51] Time-resolved studies demonstrated that fast electron transfer occurs in the subpicosecond time scale in similar directly-linked porphyrin–ferrocene dyads.[37, 52] The ultrafast timescale of the electron transfer indicates that the process occurs before solvation, which makes solvent polarity irrelevant; the process occurs even in nonpolar benzene.[52] Introduction of a ferrocene group was manifested by a new redox wave for ZnPFcPyC at +0.07 V vs ferrocenium/ferrocene, which was less positive than the purely porphyrin-based first oxidation at +0.38 V for ZnPPyC (Figure S9). (3) We expected that Förster-type energy transfer would occur among porphyrin units associated with axial coordination of a *meso*-pyridyl moiety much faster than the singlet excited state lifetime of zinc porphyrins, which was confirmed later as discussed in the last part of Results and Discussion.[19] Therefore, energy transfer from one porphyrin molecule to another in the assembly should occur many times over before decaying into the ground state. The consequence of assumptions 1–3 is that one molecule of ZnPFcPyC in the assembly would be enough to quench the fluorescence of all the other porphyrin molecules in the *n*-mer assembly. The only *n*-mer that can emit fluorescence is then $(ZnPPyC)_n$ without a ferrocene unit among various *n*-mers $(ZnPPyC)_{n-k}(ZnPPyC)_k$ ($k = 0, 1, \dots, n$). The fraction of $(ZnPPyC)_n$ among all the *n*-mers in the statistical mixture is $(1-x)^n$, when ZnFcPPyC and ZnPPyC are mixed in a ratio of x to $1-x$. We prepared chloroform solutions with varied x with the combined concentration being constant at 0.1 mM:

$$x = \frac{[\mathrm{ZnPFcPyC}]}{[\mathrm{ZnPFcPyC}] + [\mathrm{ZnPPyC}]} = \frac{[\mathrm{ZnPFcPyC}]}{0.1\ \mathrm{mM}} \qquad (2)$$

and fluorescence was measured for each solution.

Figure 3 collects the results of relevant spectroscopic studies for mixtures of ZnPPyC and ZnPFcPyC in chloroform. The absorption spectra for the mixture of ZnPPyC and ZnPFcPyC with the total concentration of 0.1 mM showed four isosbestic points at 544 nm, 578 nm, 598 nm, and 616 nm (Figure 3a). We noted that there was an irregularity around 700 nm: a peak was observed for the spectrum of ZnPPyC, which grew with time. Although the precise nature of this peak is unclear, it is likely that the fraction of molecules that is responsible for this absorption is very small, because clean isosbestic points are observed at different wavelengths and the molecules/assemblies should be stable as no new species was detected by repeated and prolonged ^{1}H NMR measurements in $CDCl_3$. Fluorescence was measured by exciting at 598 nm, one of the isosbestic points. The intensities were read at 730 nm, a long wavelength foot of the fluorescence spectra (Figure S10) to avoid the effect of reabsorption. The plot of fluorescence intensities versus x is shown in Figure 3b. Also shown in the graph are lines of $(1-x)^n$, where n is one to eight from top to bottom. The observed fluorescence intensities are on the curve of $(1-x)^3$, which supports that the assembly is a trimer.

Even though the fluorescence intensities are diminished with increasing fraction of ZnPFcPyC, the fluorescent lifetimes were found to be practically constant, 1.16 ns, 1.23 ns, and 1.31 ns for samples of x = 0, 0.2, and 0.3, respectively (Figure 3c), which is consistent with the assumption that the singlet excited state in a trimer containing a ferrocene unit is effectively quenched and the fluorescence observed is from the same species, i.e., $(ZnPPyC)_3$. The short lifetime due to quenching should be much faster than our instrument limit (<0.1 ns). This is expected on the basis of the ultrafast electron transfer in subpicosecond time scale reported for similar directly-linked porphyrin–ferrocene dyads, as mentioned earlier,[37, 52] as well as our own measurements as described later.

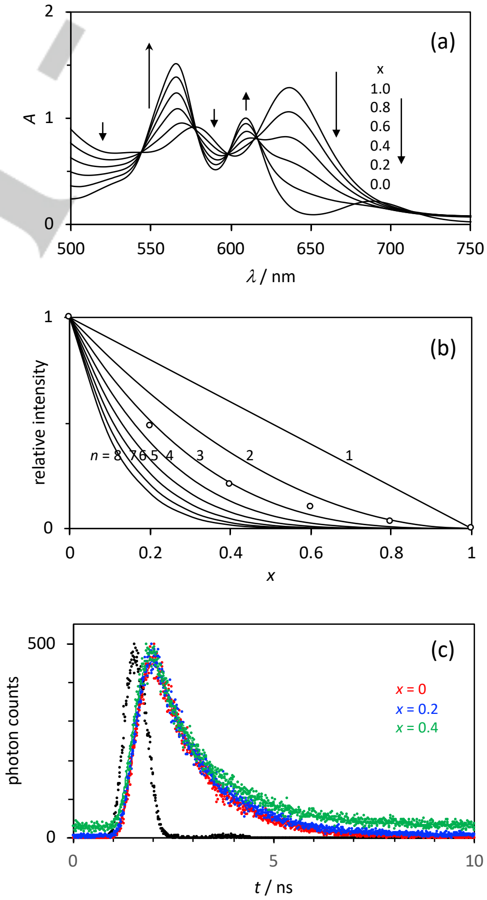

Figure 3. Spectroscopy for mixtures of ZnPPyC (fraction: $1-x$) and ZnPFcPyC (fraction: x) (combined to be 0.1 mM) in chloroform. (a) Visible absorption spectra at 25 °C. (b) Fluorescence intensity at 730 nm excited at 598 nm at 25 °C. Lines show $(1-x)^n$, with the values of n are indicated. (c) Fluorescence lifetimes at room temperature (~25 °C). The black dots represent the instrument response function.

Figure 4 depicts the system schematically. ZnPPyC and ZnPFcPyC together assemble into trimers with statistical ratios. In the assemblies containing one or two molecules of ZnPFcPyC, the ferrocene unit not only quenches the fluorescence of the porphyrin to which it is covalently bonded but also the fluorescence of the other porphyrins in the assembly, either through stepwise energy and electron transfer or through direct intermolecular electron transfer. Thus, the porphyrin chromophores work as a light-harvesting antenna in the antenna/charge separation assemblies.[53-55] We will discuss this aspect in the last part of Results and Discussion.

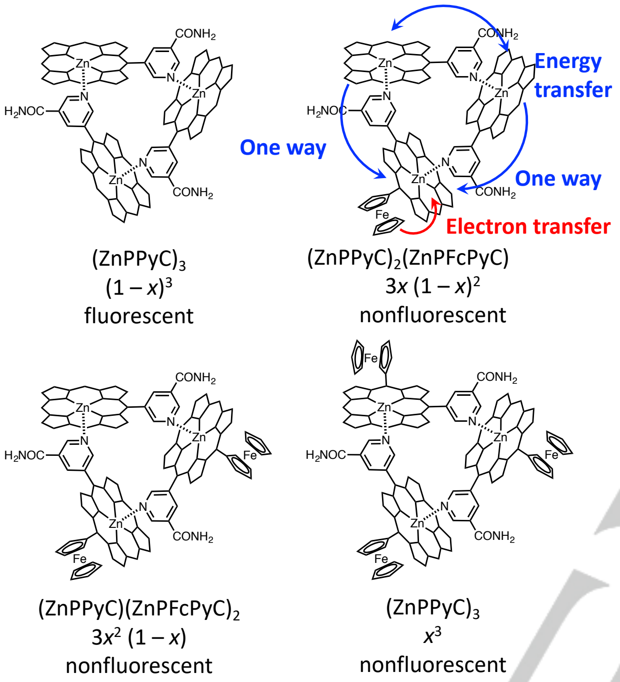

$(ZnPPyC)_3$
$(1-x)^3$
fluorescent

$(ZnPPyC)_2(ZnPFcPyC)$
$3x(1-x)^2$
nonfluorescent

$(ZnPPyC)(ZnPFcPyC)_2$
$3x^2(1-x)$
nonfluorescent

$(ZnPPyC)_3$
x^3
nonfluorescent

Figure 4. Schematic drawing of the light harvesting/charge separation model. Formulas indicate the fractions of species in the statistical mixture when [ZnPPyC]:[ZnPFcPyC] = $(1–x):x$. Energy and electron transfer pathways are indicated by curved arrows.

Structure of the trimer

So far, the data indicate that the assembly of ZnPPyC in chloroform is (1) a single species, (2) a trimer, (3) a closed structure, (4) C_3 symmetrical, i.e., all molecules are equivalent on average, (5) a structure in which the porphyrin's pseudo-mirror symmetry is lost, and (6) a structure in which porphyrins are mutually axially coordinated. Structures similar to the reported tetrameric X-ray crystal structure for a zinc *meta*-pyridyl porphyrin[29] can be excluded not only because ZnPPyC molecules form a trimer but because if that was the case there should have been a distinction of inner and outer pyridyl groups, while only one set of pyridyl protons was actually observed.

Further insight into the structure of the assembly was obtained by analyzing the chemical shits values in the ^{1}H NMR spectrum, which gives a rich information on the structure of porphyrin assemblies because of large ring-current effects of the porphyrin macrocyle. The parameters (number, magnitudes, positions, and orientations) for the magnetic dipoles equivalent to zinc porphyrin macrocycles were well established,[47, 56-57] which we used here (see Supporting Information for details). Possible supramolecular structures were searched by changing the structural parameters defined as in Figure 5a. Specifically, (1) the porphyrin center was placed on the *x*-axis away from the origin by *x*, *i.e.*, at $(x, 0, 0)$, (2) the rotation of each *meso*-substituent about the porphine–substituent bond was allowed (θ_{Pyr}, θ_{Ph1}, θ_{Ph2}, and θ_{Ph3}), (3) the orientation of the porphyrin plane was adjusted by three angles (θ, ϕ, and γ), and finally, (4) the second and third porphyrin molecules were generated by rotating ±120° about the *z*-axis. Then the ring current effects on every proton by all the aromatic systems including the porphine, phenyl, and pyridyl rings were calculated using a classical magnetic dipole model.[47, 56-57] As the one-by-one assignment of ^{1}H NMR signals to individual protons was not possible but only the categorization of peaks to the protons of porphine, pyridyl, and phenyl fragments was made, the least-squares fitting of the calculated chemical shits to the observed shifts was done on the fragment basis. In addition to the parameters listed above, effects of bending of porphine–pyridyl bond as well as the *doming* of porphyrin plane[58] were also investigated, but a distortionless, planar conformation gave the best result. Details are described in Supporting Information.

The calculated chemical shifts as a result of the least-squares fitting agreed reasonably with the observed shifts as shown in Figure 5b, while the trimer structure on which the calculated chemical shifts are based is shown in Figure 5c. The overall shape of the core part is an open triangular cone, in which three porphyrin molecules constitute the three faces and the remaining face is open. This core part is highlighted in Figure 5d, in which the triangular cone is shown from the open side and from the tip side, both along the C_3 axis towards the reader.

The calculated shifts from the trimer model reproduced some key points. First, upfield shifts of pyridyl protons ortho to the nitrogen, both large but to significantly different degrees were reproduced. It is now possible to assign the most upfield (2.11 ppm) and the second upfield (3.37 ppm) shifts to the 3- and 1-protons of the pyridyl moiety. The different degrees of the upfield shifts are due to the offset, slanted axial coordination of the pyridyl moiety to the zinc ion. Second, the lowered symmetry was also reproduced, with individual proton signals appearing separately one by one, not necessarily as a multiple of two protons. This is due to the cone shape in which the pseudo-mirror plane through the pyridyl-porphine bond is lost. Third, an exceptionally large upfield shift (5.13 ppm) of one porphine proton was reproduced, allowing its assignment to the 2-proton of the porphine core, which is adjacent to the pyridyl moiety in the narrow side of the cone, which is the closest to another porphyrin macrocycle. A discrepancy was noted on a set of phenyl protons at 5.37 ppm and 5.99 ppm, which were *J*-coupled according to the COSY result. One proton (proton-12) appeared nearby at 5.61 ppm but the *J*-coupled counterpart (proton-11), appeared at 8.86 ppm by calculation. Proton-11 and proton-12 are protons on the phenyl moieties clogging at the tip of the cone, which are seen in the center region of the lower model of Figure 5d. Thus, it is likely that their chemical shifts are quite sensitive to a slight movement about the C_3 axis passing through the tip of the triangular cone, which may account for the discrepancy of the calculated chemical shift value of proton-11. Finally, it is seen that carbamoyl moiety is not involved in any intermolecular interaction in the trimer.

10.1002/chem.202003327

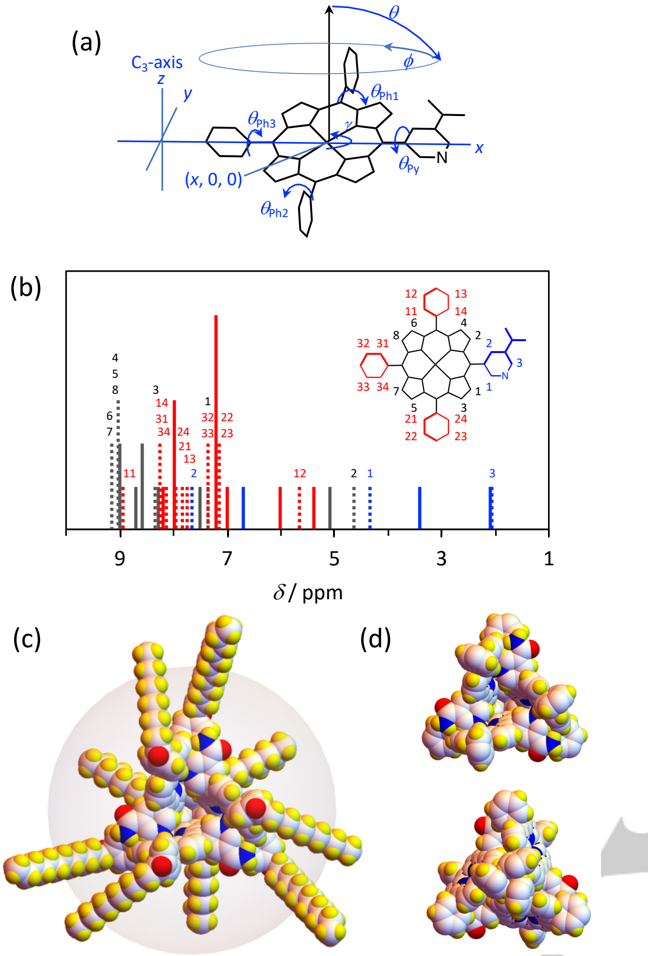

Figure 5. Trimer model which accounts for the observed ^{1}H NMR spectrum in CDCl$_3$. (a) Parameters to be optimized. (b) Observed (solid lines) and calculated (dotted lines) chemical shits. (c) NMR-fitted trimer θ_{Py} = 163°, θ_{Ph1} = –3°, θ_{Ph2} = –1°, θ_{Ph3} = 4°, x = 4.98 Å, θ = 72.5°, ϕ = –140.7°, γ = 117.3°. Dodecyloxy chains are put in arbitrary orientations. The hydrodynamic sphere (gray) obtained from the DOSY is superimposed. (d) Dodecyloxy groups are omitted to highlight the core part. The upper is a view from the open side (inner surface) and the lower is a view from the tip side (outer surface).

We checked if an energy-minimized structure was found in the triangular cone structure by semiempirical quantum mechanical calculations using the PM6 method,[59] which has been applied to axially-coordinated zinc porphyrin systems.[60] The optimized structure is shown in Figures 6 and S11. The overall, near C$_3$ structure is similar to the one obtained from the ring-current simulation. Some distortions are observed to realize three coordination bonds in the congested region. Most prominently, the pyridyl moieties are warped with respect to the porphine plane; the angles made by the porphine plane and the pyridyl C2–C5 axis (C2 and C5 are the farthest and closest carbon atoms from the porphine ring) are 18.8°–19.2°. In addition, the pyridyl ring is rotated from the orthogonal orientation with respect to the porphine plane by 28–31°. Further, the ligand axes (pyridyl N–C4 axis) are slanted with respect to the coordinated porphine planes, by 10.1°–10.2°. Apparently, synergy of the triple coordination bond formation outweighs these higher energy distortions in the supramolecular conformations, resulting in the trimer, which are stable in a wide concentration and temperature ranges.

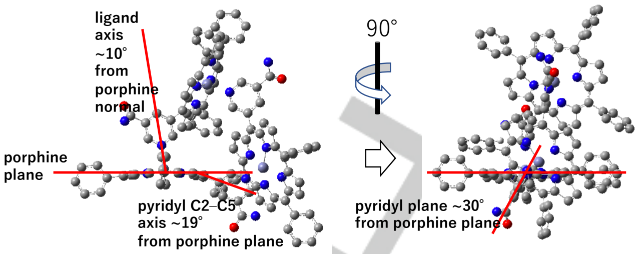

Figure 6. Distortion seen in the PM6-optimized trimer structure. The alkoxy chains were replaced by hydrogen atoms in the calculation. Hydrogen atoms are omitted for clarity in the drawing.

Photosynthetic Antenna/Reaction Center Model

As the supramolecular trimer structure has been revealed, the rate of Förster energy transfer among porphyrins in the trimer was estimated based on the structural information according to the formula (see Supporting Information for details including the definitions of variables):[61]

$$k_{\text{Förster}} = \frac{9(\ln 10)\kappa^2\Phi_{\text{f}}}{128\pi^5 n^4 r^6 N_{\text{A}}\tau_{\text{D}}}\,\frac{\int d\lambda\,\lambda^4 F_{\text{D}}(\lambda)\varepsilon_{\text{A}}(\lambda)}{\int d\lambda\,F_{\text{D}}(\lambda)} \qquad (3)$$

The calculations indicate that the energy transfer from one ZnPPyC to another ZnPPyC occurs in 7.0 ps and that from ZnPPyC to ZnPFcPyC occurs in 8.1 ps. These values are shorter that the singlet excited state lifetime of 1.2 ns more than two-orders of magnitude. Interestingly, the back energy transfer rate from ZnPFcPyC to ZnPPyC is expected to be negligibly small because (1) the fluorescence yield of ZnPFcPyC is negligibly small (≲1% compared to ZnPPyC) and (2) the singlet excited state energy of ZnPFcPyC (1.92 eV) is lower than that of ZnPPyC (2.00 eV) as estimated from the absorption (Figure 3a) and fluorescence spectra (Figure S10). For a trimer containing both ZnPPyC and ZnPFcPyC, once ZnPPyC absorbs a photon, efficient energy transfer to another porphyrin occurs. While energy transfer between ZnPPyC molecules are reversible, energy transfer from ZnPPyC to ZnPFcPyC is one way.

Subsequently, the singlet excited state of ZnPFcPyC is quickly quenched by a process involving the ferrocene moiety. To obtain insight into this fast process, we conducted femtosecond transient absorption measurements. Figure 7a shows the transient absorption spectra during the initial 200 ps duration after excitation of ZnPFcPyC by a laser with a pulse width of ~35 fs. The ground-state bleaching at ~580 nm and ~650 nm corresponds to the Q-bands of ZnPFcPyC. The broad absorption feature was observed to the low energy side of the bleach, which may be assigned to the zinc-porphyrin radical anion.[37, 52, 62] Transient absorption spectra of ZnPFcPyC were fitted with three decay components and the time trances at two representative wavelengths are shown in Figure 7b.

The fast relaxation process can represent the formation of the charge-separated state, but the exact time constant for this subpicosecond process could not be determined because it was shorter than our instrumental resolution. The time constant of 2.3 ps could represent the conformation changes after the formation of the charge-separated state. The longest time component of 26 ps indicates the charge recombination process. These assignments are fully consistent with the literature for the above

10.1002/chem.202003327

mentioned directly-linked porphyrin-ferrocene dyads[37, 52] and none of these fast processes was present for ZnPPyC without the ferrocene unit (Figure S12).

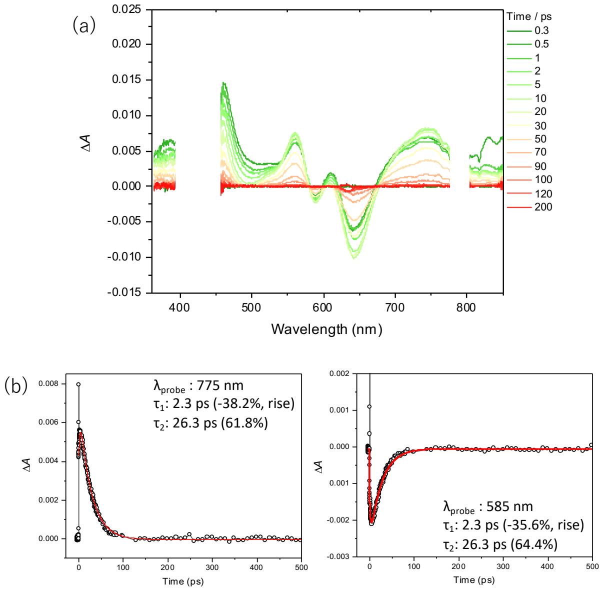

Figure 7. Femtosecond transient absorption for ZnPFcPyC in toluene. (a) Transient spectra. (b) Time traces at 775 nm and 585 nm.

The energies of the resulting intramolecular charge-separated state was estimated to be 2.07 eV by using the Weller equation, on the assumption that the positive and negative charges are localized on the ferrocene and porphyrin sites, respectively (see Supporting Information for details including the definitions of variables):

$$E = e\left\{E_{\mathrm{ox}} - E_{\mathrm{red}} - \frac{e}{4\pi\varepsilon_{\mathrm{r}}\varepsilon_0 r}\right\} \quad (4)$$

This value (2.07 eV) is slightly larger than the singlet excited state energy of ZnPFcPyC (1.92 eV). This may be due to approximations involved in the estimation from combination of different methods, *i.e.*, electrochemistry and spectroscopy. Particularly, it is likely that the charges are delocalized over the ferrocene unit and porphyrin unit, lowering the energy of the charge-separated state.[37] In the meantime, energies of various intermolecular charge-separated states, *e.g.*, $(\mathrm{ZnPPyC})^{\bullet-}$ $(\mathrm{ZnPFcPyC})^{\bullet+}$, were all found to be higher than the intramolecular charge-separated state (Table S3). Thus, the trimer consisting of ZnPPyC and ZnPFcPyC represents a complex of a light-harvesting antenna with an energy gradient and a charge separation reaction center.

Conclusion

We have investigated the self-assembly of some zinc *meso*-(*meta*-pyridyl)porphyrins. Among them, one with a carbamoyl group on the pyridyl moiety, ZnPPyC, was found to give a distinct ^{1}H NMR spectrum in $CDCl_3$ which allowed us to investigate the structure in solution in detail. The ^{1}H NMR spectra were nearly unaltered over a wide range of temperatures from –50 °C to +50 °C and a wide range of concentrations from 0.1 mM to 5 mM. The formation of assembly was evidenced by an increased hydrodynamic radius twice as large as that of a monomer. This molecule could have had either one of the two motifs of assembly. In one, hydrogen bonding and axial coordination synergistically produce shallowly angled (30°) porphyrin association that would lead to a large ring structure, which is reminiscent of the light-harvesting antenna in purple bacteria. In the other, a smaller ring would result if axial coordination dominates and hydrogen bonding was not involved. Molecular weight determination by vapor pressure osmometry indicated that the assembly was a trimer. The results presented here excluded the possibility of a large ring formation. Simulation of ring-current-induced chemical shift changes indicated that the structure of the trimer was a triangular cone, of which the three faces were occupied by the porphyrin molecules and the remaining one face open.

A ferrocene-containing molecule, ZnPFcPyC, with the same intermolecular interaction units was mixed with ZnPPyC to generate statistical mixtures containing both the sensitizer units and charge-separation units. The quenching experiment not only confirmed that the assembly was a trimer but exemplified a rare system of light-harvesting antenna/charge separation complexes in which an energy gradient is incorporated and reductive quenching occurred very efficiently (practically 100% efficiency). We have previously reported a light-harvesting antenna/charge separation system, which resulted from a statistical assembly of a fluorescent chlorophyll derivative and a nonfluorescent chlorophyll–fullerene conjugate.[26] As the fullerene unit oxidatively quenches the fluorescence, the present system is a complementary system, in the sense that the porphyrin fluorescence is reductively quenched.

Directing assembly of porphyrin molecules toward a larger antenna such as the light-harvesting antennas in purple bacteria and the one shown on the right in Figure 1 is a fascinating challenge. We can draw some lessons from this work to realize a large ring-like antenna structure based on improvement of the present design. Here we have seen that axial coordination dominates over hydrogen bonding. Hence, one way may be to use a stronger auxiliary interaction by making modification on the part of the carbamoyl moiety. We have also seen that three axial bonds are realized by a congested region with forced distortions. Therefore, another way to direct the assembly towards the large ring formation may be to hinder the distortion, say, by introducing substituents on or around the pyridyl moiety to restrict its rotation. These lines of attempts are underway in our laboratory.

Experimental Section

Thin layer chromatography (TLC) was performed on Merck silica gel 60F254. Flash column chromatography was performed using Kanto Chemical silica gel (SiO_2) 60N. Recycle gel permeation chromatography (GPC) was conducted, using $CHCl_3$ as the eluent, on a Japan Analytical Industry LC-9201 system equipped with Jaigel-2H and Jaigel-1H columns in tandem, with exclusion limits of 5000 and 1000, respectively. NMR spectra were recorded with a JEOL JNM-ECX400 NMR spectrometer (400 MHz for 1H and 100 MHz for ^{13}C). Laser-desorption (LDI)-HRMS data were recorded with a JMS-S3000 MS spectrometer. The spectra were calibrated with a mixture of 4-methoxy-*N*-phenylbenzenamine (M^+

($C_{13}H_{13}NO$) 199.0992), *meso*-tetraphenylporphyrin (MH$^+$ ($C_{44}H_{31}N_4$), 615.2543) and Zn *meso*-tetrakis(*p*-dodecyloxyphenyl)porphyrin (MH$^+$ ($C_{92}H_{127}N_4O_4$), 1351.9852). Vapor pressure osmometry measurement was conducted for samples dissolved in $CHCl_3$ stabilized with amylene at 45 ºC using a Gonotec Osmomat 070 osmometer. The calibration curve was made using benzil as the standard. DOSY experiments were carried out on a JEOL JNM-ECA500 or JNM-ECX400 spectrometer using a bipolar pulse pair stimulated echo pulse sequence. Visible absorption and fluorescence spectra were measured on Jasco V-770 and FP-8600 spectrometers, respectively. Fluorescence lifetimes were measured on a Hamamatsu Quantaurus-Tau C11367. Cyclic voltammetry was conducted on an ALS/CH Instruments electrochemical analyzer 608DN. The working, counter, and pseudo reference electrodes were glassy carbon, Pt coil, and Ag wire, respectively. The sample (1 mM) was dissolved in 0.1 M tetrabutylammonium hexafluorophosphate solution in 1,2-dichloroethane. The scan rate was 100 mV s^{-1}. The potentials were calibrated against internal ferrocene added after each measurement. Transient absorption measurements were conducted using a dual-beam femtosecond time-resolved transient absorption spectrometer consisted of two independently-tunable home-made noncollinear optical parametric amplifiers pumped by a regeneratively amplified Ti:sapphire laser system (Spectra-Physics, Hurricane-X) operating at 3 kHz repetition rate and an optical detection system. For more details for transient absorption, see Supporting Information.

H_2PPy. A solution of *p*-dodecyloxybenzaldehyde[63] (3.61 g, 12.4 mmol), 3-pyridinecarboxaldehyde (442 mg, 4.13 mmol), and pyrrole (1.11 g, 16.5 mmol) in propionic acid (90 mL) were refluxed in an open flask covered with aluminum foil for 2.5 h. The solvent was evaporated and the residue was dissolved in $CHCl_3$, which was washed with aqueous $NaHCO_3$ twice and aqueous NaCl once, dried over Na_2SO_4, filtered, and evaporated. The crude material was chromatographed twice (SiO_2, $CHCl_3$) and further purified with GPC to afford a purple solid (159 mg, 0.136 mmol, 3,3%). R_f = 0.4 (SiO_2, $CHCl_3$); ^{1}H NMR ($CDCl_3$): δ = 9.45 (s, 1H), 9.03 (d, *J* = 3.7 Hz, 1H), 8.92 (d, *J* = 4.3 Hz, 2H), 8.89 (s, 4H), 8.76 (d, *J* = 4.9 Hz, 2H), 8.51 (dt, *J* = 7.3 Hz, 4.3 Hz, 1H), 8.11 (d, *J* = 7.9 Hz, 6H), 7.74 (dd, *J* = 7.3, 5.5 Hz, 1H), 7.28 (d, *J* = 8.5 Hz, 6H), 4.25 (t, *J* = 6.7 Hz, 6H), 1.98 (quintet, *J* = 7.0 Hz, 6H), 1.63 (quintet, *J* = 7.0 Hz, 6H), 1.2–1.5 (48H), 0.90 (t, *J* = 6.7 Hz, 9H), –2.76 (s, 2H) ppm; HRMS (LDI): *m*/*z* calcd for $C_{79}H_{101}N_5O_3$+H$^+$: 1168.7977 [*M*+H]$^+$; found: 1168.7927.

ZnPPy. A combined solution of H_2PPy (63 mg, 0.054 mmol) in $CHCl_3$ (4.7 mL) and $Zn(OAc)_2•(H_2O)_2$ (59 mg, 0.27 mmol) in MeOH (1.2 mL) was stirred at room temperature in the dark for 2 h. The solvents were evaporated and the residue was dissolved in $CHCl_3$, which was washed with H_2O three times, dried over Na_2SO_4, filtered, and evaporated. The crude product was crystallized from $CHCl_3$/MeCN to afford a purple solid (49 mg, 0.040 mmol, 74%). R_f = 0.55 (SiO_2, $CHCl_3$/pyridine 95:5); ^{1}H NMR ($CDCl_3$): a broad spectrum, see text. HRMS (LDI): *m*/*z* calcd for $C_{79}H_{99}N_5O_3Zn^+$ [*M*]$^+$: 1229.7034; found: 1229.7080.

H_2PPyA. A solution of *m*-octyloxybenzaldehyde[64] (316 mg, 1.35 mmol), 5-acetamido-3-pyrydinecarboxaldehyde[65] (76 mg, 0.46 mmol), and pyrrole (123 mg, 1.84 mmol) in propionic acid (8 mL) was refluxed in an open flask covered with aluminum foil for 2.5 $CHCl_3$, which was washed with aqueous $NaHCO_3$ three times, dried over Na_2SO_4, filtered, and evaporated. The crude material was chromatographed (SiO_2, $CHCl_3$ → $CHCl_3$/MeOH 98:2) and further purified by GPC to afford a purple solid (61 mg, 0.058 mmol, 13%). R_f = 0.45 (SiO_2, $CHCl_3$/MeOH 9:1); ^{1}H NMR ($CDCl_3$): δ = 9.18 (br, 1H), 9.08 (br, 1H), 8.94 (d, *J* = 4.9 Hz, 2H), 8.90 (s, 5H), 8.81 (d, *J* = 4.9 Hz, 2H), 7.75–7.8 (6H), 7.63 (t, *J* = 7.9 Hz, 3H), 7.56 (s, 1H), 7.33 (dd, *J* = 8.5 Hz, 1.8 Hz, 3H), 4.14 (t, *J* = 6.7 Hz, 6H), 2.29 (s, 3H), 1.87 (quintet, *J* = 6.7 Hz, 6H), 1.50 (quintet, *J* = 7.9 Hz, 6H), 1.2–1.4 (24H), 0.85 (t, *J* = 6.7 Hz, 9H), –2.83 ppm (s, 2H); HRMS (LDI): *m*/*z* calcd for $C_{69}H_{80}N_6O_4$+H$^+$: 1057.6314 [*M*+H]$^+$; found: 1057.6225.

ZnPPyA. A combined solution of H_2PPyA (60 mg, 0.06 mmol) in $CHCl_3$ (7 mL) and $Zn(OAc)_2$ (60 mg, 0.33 mmol) in MeOH (3.5 mL) was stirred at rt for 4 h. The solvents were evaporated and the residue was redissolved in $CHCl_3$, which was washed with H_2O three times, dried over Na_2SO_4, filtered, and evaporated. The obtained material was further dried under vacuum to afford a purple solid (60 mg, 0.06 mmol, 100%). R_f = 0.5 (SiO_2, $CHCl_3$/MeOH 9:1); HRMS (LDI): *m*/*z* calcd for $C_{69}H_{78}N_6O_4Zn^+$: 1118.5371 [*M*]$^+$; found: 1118.5284.

H_2PPyCO$_2$Me. A solution of *p*-dodecyloxybenzaldehyde[63] (10.8 g, 37.2 mmol), methyl 5-formyl-3-pyridinecarboxylate[66-67] (2.05 g, 12.4 mmol), and pyrrole (3.32 g, 49.6 mmol) in propionic acid (200 mL) was refluxed in an open flask covered with aluminum foil for 2.5 h. The solvent was evaporated and the residue was dissolved in $CHCl_3$, which was washed with aqueous $NaHCO_3$ twice and with aqueous NaCl once, dried over Na_2SO_4, filtered, and evaporated. The crude material was chromatographed (SiO_2, $CHCl_3$) twice to afford a purple solid (1.20 g, 0.983 mmol, 7.9%). R_f = 0.5 (SiO_2, $CHCl_3$); ^{1}H NMR ($CDCl_3$): δ = 9.65 (d, *J* = 1.8 Hz, 1H), 9.60 (d, *J* = 2.4 Hz, 1H), 9.11 (t, *J* = 2.1 Hz, 1H), 8.94 (d, *J* = 4.9 Hz, 2H), 8.89 (s, 4H), 8.69 (d, *J* = 4.9 Hz, 2H), 8.11 (d, *J* = 8.5 Hz, 6H), 7.28 (d, *J* = 8.5 Hz, 6H), 4.25 (t, *J* = 6.7 Hz, 6H), 4.05 (s, 3H), 1.98 (quintet, *J* = 7.3 Hz, 6H), 1.63 (quintet, *J* = 7.3 Hz, 6H), 1.3–1. 5 (m, 48H), 0.90 (t, *J* = 6.7 Hz, 9H), –2.76 ppm (s, 2H); HRMS (LDI): *m*/*z* calcd for $C_{81}H_{103}N_5O_5$+H$^+$: 1226.8032 [*M*+H]$^+$; found: 1226.8038.

H_2PPyCO$_2$H. A combined solution of H_2PPyCO$_2$Me (1.20 g, 0.909 mmol) in THF (190 mL) and KOH (5.09 g) in H_2O (3 mL) was refluxed in a flask capped by a balloon and covered with aluminum foil for 14 h. THF was evaporated and the remaining aqueous layer was neutralized with 1 M HCl. The aqueous layer was extracted with $CHCl_3$, which was dried over Na_2SO_4, filtered, and evaporated. The crude material was chromatographed (SiO_2, $CHCl_3$/MeOH 95:5) to afford a purple solid (1.17 g) including some impurities, which was used for the subsequent reaction. R_f = 0.2 (SiO_2, $CHCl_3$/MeOH 9:1); ^{1}H NMR ($CDCl_3$): δ = 9.57 (br, 2H), 8.86 (br, 7H), 8.62 (br, 2H), 8.06 (br, 6H), 7.22 (br, 6H), 4.23 (br, 6H), 1.93 (br, 6H), 1.58 (br, 6H), 1.2–1.5 (48H), 0.89 (m, 9H), –2.75 ppm (2H), CO_2H not identified; HRMS (LDI): *m*/*z* calcd for $C_{80}H_{101}N_5O_5$+H$^+$: 1212.7842 [*M*+H]$^+$; found: 1212.7839.

H_2PPyC. A solution of H_2PPyCO$_2$H (1.17 g, 0.967 mmol) and carbonyldiimidazole (CDI, 1.57 g, 9.67 mmol) in dry THF (100 mL) was refluxed under N_2 for 1 h. After the solution was cooled to room temperature, aqueous NH_3 (28–30%, 14 mL) was added and the solution was further stirred under N_2 in the dark for 21 h. The solution was concentrated to about a half volume to which CHCl3 (200 mL) was added. The solution was washed with aqueous $NaHCO_3$ three times, dried over Na_2SO_4, filtered, and evaporated. The crude material was chromatographed twice (SiO_2, $CHCl_3$ → $CHCl_3$/MeOH 96:4 and SiO_2, $CHCl_3$ → $CHCl_3$/MeOH 98:2) and further purified by GPC to afford a purple solid (829 mg, 0.685 mmol, 71%). R_f = 0.6 (SiO_2, $CHCl_3$/MeOH 9:1); ^{1}H NMR ($CDCl_3$): δ = 9.59 (d, *J* = 1.8 Hz, 1H), 9.40 (d, *J* = 2.4 Hz, 1H), 8.85–8.95 (7H), 8.69 (d, *J* = 4.9 Hz, 2H), 8.05–8.15 (6H), 7.2–7.3 (6H), 6.26 (br, 1H), 5.79 (br, 1H), 4.2–4.3 (6H), 1.9–2.0 (6H), 1.55–1.65 (6H), 1.2–1.5 (48H), 0.90 (t, *J* = 6.7 Hz, 9H), –2.76 ppm (s, 2H); HRMS (LDI): *m*/*z* calcd for $C_{80}H_{102}N_6O_4$+H^+: 1211.8035 [*M*+H]$^+$; found: 1211.7998.

ZnPPyC. A combined solution of H_2PPyC (769 mg, 0.636 mmol) in $CHCl_3$ (60 mL) and $Zn(OAc)_2$•$(H_2O)_2$ (696 mg, 3.18 mmol) in MeOH (15 mL) was stirred at room temperature in the dark for 3 h. The solvents were evaporated and the residue was dissolved in $CHCl_3$, which was washed with H_2O three times, dried over Na_2SO_4, filtered, and evaporated. The crude product was chromatographed twice (SiO_2, $CHCl_3$/MeOH 98:2) to afford a purple/green solid (716 mg, 0.562 mmol, 88%). R_f = 0.45 (SiO_2, $CHCl_3$/MeOH 95:5); ^{1}H NMR ($CDCl_3$): δ = 8.99 (d, *J* = 4.9 Hz, 1H), 8.96 (d, *J* = 4.9 Hz, 1H), 8.70 (d, *J* = 4.9 Hz, 1H), 8.55–8.65 (2H), 8.34 (d, *J* = 4.3 Hz, 1H), 8.18 (d, *J* = 7.9 Hz, 1H), 8.0–8.1 (2H), 7.98 (d, *J* = 6.7 Hz, 1H), 7.72 (d, *J* = 7.9 Hz, 1H), 7.51 (d, *J* = 4.9 Hz, 1H), 7.15–7.25 (4H), 6.93 (d, *J* = 6.7 Hz, 1H), 6.68 (s, 1H), 6.28 (br, 1H), 6.00 (d, *J* = 7.9 Hz, 1H), 5.37 (d, *J* = 7.3, 1H), 5.13 (d, *J* = 3.7 Hz, 1H), 4.15–4.25 (4H), 3.93 (br, 1H), 3.4–3.6 (m, 2H), 3.37 (s, 1H), 2.11 (br, 1H), 1.9–2.0 (m, 4H), 1.15–1.7 (56H), 0.8–0.95 ppm (9H); HRMS (LDI): *m*/*z* calcd for $C_{80}H_{100}N_6O_4Zn^+$: 1272.7092 [*M*]$^+$; found: 1272.7175.

H_2PFcPyCO$_2$Me. A mixture of *meso*-(4-dodecyloxytphen-1-yl)-2,2'-dipyrromethane[68] (6.74 g, 16.6 mmol), methyl 5-formyl-3-pyridinecarboxylate[66-67] (1.37 g, 8.30 mmol), ferrocenecarboxaldehyde (1.78 g, 8.30 mmol), and NH_4Cl (8.88 g, 166 mmol) in CH_2Cl_2 (1.65 L) in a flask capped with a septum was deoxygenated by bubbling N_2 for 20 min. TFA (2.5 mL, 33 mmol) was added through the septum to the mixture, which was stirred at room temperature in the dark for 4 h. DDQ (5.65 g, 24.9 mmol) was then added and the mixture was further stirred at room temperature for 14 h. Finally, Et_3N (4.62 mL, 33.2 mmol) was added and the solution was concentrated to ~500 mL, which was passed through a pad of SiO_2. The fractions containing the desired compound were chromatographed twice (SiO_2, $CHCl_3$ → $CHCl_3$/MeOH 99:1 and $CHCl_3$). The collected fractions still contained H_2PPyCO$_2$Me, which was removed by GPC to afford a purple solid (285 mg, 0.248 mmol, 3.0%). R_f = 0.7 (SiO_2, $CHCl_3$/MeOH 99:1); ^{1}H NMR ($CDCl_3$): δ = 10,00 (d, *J* = 4.3 Hz, 2H), 9.63 (d, *J* = 1,8 Hz, 1H), 9.57 (d, *J* = 2.4 Hz, 1H), 9.09 (t, *J* = 2.4 Hz, 1H), 8.84 (d, *J* = 4.9 Hz, 2H), 8.82 (d, *J* = 4.9 Hz, 2H), 8.62 (d, *J* = 4.9 Hz, 2H), 8.10 (d, *J* = 8.5 Hz, 4H), 7.29 (d, *J* = 8.5 Hz, 4H), 5.57 (m, 2H), 4,.86 (m, 2H), 4.26 (t, *J* = 7.3 Hz, 4H), 4.19 (s, 5H), 4.06 (s, 3H), 1.99 (quintet, *J* = 7.3 Hz, 4H), 1.64 (quintet, *J* = 7.3 Hz, 4H), 1.25–1.55 (32H), 0.90 (t, *J* = 0.89 Hz, 6H), –2.30 ppm (s, 2H); HRMS (LDI): *m*/*z* calc for $C_{73}H_{83}FeN_5O_4$+H^+: 1150.5867 [*M*+H]$^+$; found: 1150.5932.

H_2PFcPyCO$_2$H. A combined solution of H_2PFcPyCO$_2$Me (277 mg, 0.241 mmol) in THF (33 mL) and KOH (1.41 g, 25.2 mmol) in H_2O (0.82 mL) was refluxed in a flask capped by a balloon and covered with aluminum foil for 15 h. THF was evaporated and the remaining aqueous layer was neutralized with 1 M HCl and extracted with $CHCl_3$, which was dried over Na_2SO_4, filtered, and evaporated. The crude material was chromatographed (SiO_2, $CHCl_3$ → $CHCl_3$/MeOH 9:1) to afford a purple solid (253 mg, 0.223 mmol, 93%). R_f = 0.25 (SiO_2, $CHCl_3$/MeOH 9:1); ^{1}H NMR ($CDCl_3$): δ = 9.98 (br, 2H), 9.54 (br, 2H), 8.81 (br, 5H), 8.58 (br, 2H), 8.08 (br, 4H), 7.2 (br, 4H), 5.58 (br, 2H), 4.86 (br, 2H), 4.24 (br, 4H), 4.18 (s, 5H), 1.2–2.0 (40H),0.90 (t, *J* = 7.3 Hz, 6H), –2.30 ppm (br, 2H); HRMS (LDI): *m*/*z* calc for $C_{72}H_{81}FeN_5O_4$+H^+: 1136.5711 [*M*+H]$^+$; found: 1136.5630.

H_2PFcPyC. A solution of H_2PFcPyCO$_2$H (243 mg, 0.214 mmol) and carbonyldiimidazole (CDI, 347 mg, 2.14 mmol) in dry THF (22 mL) was refluxed under N_2 for 1 h. After the solution was cooled to room temperature, aqueous NH_3 (28–30%, 14 mL) was added and the solution was further stirred under N_2 in the dark for 17 h. The solution was diluted with $CHCl_3$ which was washed with aqueous $NaHCO_3$ three times, dried over Na_2SO_4, filtered, and evaporated to afford a purple solid, which was essentially pure (237 mg, 0.209 mmol, 98%). R_f = 0.6 (SiO_2, $CHCl_3$/MeOH 9:1); ^{1}H NMR ($CDCl_3$): δ = 9.99 (d, *J* = 4.3 Hz, 2H), 9.57 (d, *J* = 2.4 Hz, 1H), 9,43 (d, *J* = 2.4 Hz, 1H), 8.90 (t, *J* = 2.4 Hz, 1H), 8.84 (d, *J* = 4.9 Hz, 2H), 8.82 (d, *J* = 5.5 Hz, 2H), 8.63 (d, *J* = 4.9 Hz, 2H), 8.10 (d, *J* = 8.5 Hz, 4H), 7.29 (d, *J* = 8.5 Hz, 4H), 6.32 (br, 1H), 5.79 (br, 1H), 5.57 (m, 2H), 4.86 (m, 2H), 4.26 (t, *J* = 6.7 Hz, 4H), 4.19 (s, 5H), 1.99 (quintet, *J* = 6.7 Hz, 4H), 1.63 (quintet, *J* = 7.9 Hz, 4H), 1.25–1.50 (32H), 0.90 (t, *J* = 6.7 Hz, 6H), –2.30 ppm (s, 2H). HRMS (LDI): *m*/*z* cald for $C_{72}H_{82}FeN_6O_3$+H^+: 1135.5871 [*M*+H$^+$]; found: 1135.5710.

ZnPFcPyC. A combined solution of H_2PFcPyC (237 mg, 0.209 mmol) in $CHCl_3$ (18 mL) and Zn(OAc)•$(H_2O)_2$ (230 mg, 1.05 mmol) in MeOH (3.4 mL) was stirred at room temperature in the dark for 2 h. The solution was diluted with $CHCl_3$, which was washed with H_2O three times, dried over Na_2SO_4, filtered, and evaporated. The crude product was chromatographed twice (SiO_2, $CHCl_3$ → $CHCl_3$/MeOH 98:2) to afford a purple solid (237 mg, 0.198 mmol, 95%). R_f = 0.6 (SiO_2, $CHCl_3$/MeOH 9:1); ^{1}H NMR ($CDCl_3$): peaks are resolved but broad, see the spectrum in Supporting Information; HRMS (LDI): *m*/*z* calcd for $C_{72}H_{80}FeN_6O_3Zn^+$: 1196.4927 [*M*]$^+$; found: 1196.4866.

Acknowledgements

We thank K. Wada and M. Kudo of Center for Creative Materials Research, Research Institute of College of Science and Technology, Nihon University for low-temperature NMR and precise-weight sampling, respectively. We also thank Y. Kida for experimental help. J.O. acknowledges financial support from Kakenhi (18K05156), MEXT, Japan for part of the work. The work at Yonsei University (transient absorption) was supported by the National Research Foundation of Korea (NRF) grant funded by the Korea government (MSIT) (No. 2020R1A5A1019141).

Keywords: axial coordination • light-harvesting antenna • porphyrinoids • ring current • self-assembly

[1] *Handbook of Porphyrin Science*, *Vol.* 1 (Eds.: K. M. Kadish, K. M. Smith, R. Guilard), World Scientific, **2010**.
[2] N. Aratani, D. Kim, A. Osuka, *Acc. Chem. Res.* **2009**, *42*, 1922–1934.
[3] S. Fukuzumi, K. Ohkubo, *Dalton Trans.* **2013**, *42*, 15846–15858.
[4] J. Otsuki, *J. Mater. Chem. A* **2018**, *6*, 6710–6753.
[5] J. A. Wytko, R. Ruppert, C. Jeandon, J. Weiss, *Chem. Commun.* **2018**, *54*, 1550–1558.
[6] J. Min Park, J. H. Lee, W.-D. Jang, *Coord. Chem. Rev.* **2020**, *407*, 213157.
[7] S. Kundu, A. Patra, *Chem. Rev.* **2017**, *117*, 712–757.
[8] H. Song, Q. Liu, Y. Xie, *Chem. Commun.* **2018**, *54*, 1811–1824.
[9] A. Mahmood, J.-Y. Hu, B. Xiao, A. Tang, X. Wang, E. Zhou, *J. Mater. Chem. A* **2018**, *6*, 16769–16797.

10.1002/chem.202003327

[10] K. Zeng, Z. Tong, L. Ma, W.-H. Zhu, W. Wu, Y. Xie, *Energy Environ. Sci.* **2020**, *13*, 1617–1657.
[11] S. Shao, V. Rajendiran, J. F. Lovell, *Coord. Chem. Rev.* **2019**, *379*, 99–120.
[12] N. Takeshima, K. Sugawa, H. Tahara, S. Jin, H. Wakui, M. Fukushima, K. Tokuda, S. Igari, K. Kanakubo, Y. Hayakawa, R. Katoh, K. Takase, J. Otsuki, *ACS Nano* **2019**, *13*, 13244–13256.
[13] K. Sugawa, K. Uchida, N. Takeshima, S. Jin, N. Tsunenari, H. Takeda, Y. Kida, T. Akiyama, J. Otsuki, K. Takase, S. Yamada, *Nanoscale* **2016**, *8*, 15467–15472.
[14] K. Sugawa, N. Takeshima, K. Uchida, H. Tahara, S. Jin, N. Tsunenari, T. Akiyama, Y. Kusaka, N. Fukuda, H. Ushijima, Y. Tsuchido, T. Hashimoto, T. Hayashita, J. Otsuki, *J. Mater. Chem. C* **2015**, *3*, 11439–11448.
[15] *Multiporphyrin Arrays, Fundamentals and Applications*, (Eds.: D. Kim), Pan Stanford, **2012**.
[16] J. A. A. W. Elemans, R. v. Hameren, R. J. M. Nolte, A. E. Rowan, *Adv. Mater.* **2006**, *18*, 1251–1266.
[17] E. Iengo, E. Zangrando, E. Alessio, *Eur. J. Inorg. Chem.* **2003**, *2003*, 2371–2384.
[18] M. M. Yatskou, R. B. M. Koehorst, H. Donker, T. J. Schaafsma, *J. Phys. Chem. A* **2001**, *105*, 11425–11431.
[19] M. M. Yatskou, R. B. M. Koehorst, A. van Hoek, H. Donker, T. J. Schaafsma, B. Gobets, I. van Stokkum, R. van Grondelle, *J. Phys. Chem. A* **2001**, *105*, 11432–11440.
[20] G. Ercolani, M. Ioele, D. Monti, *New J. Chem.* **2001**, *25*, 783–789.
[21] M. M. Yatskou, H. Donker, E. G. Novikov, R. B. M. Koehorst, A. van Hoek, V. V. Apanasovich, T. J. Schaafsma, *J. Phys. Chem. A* **2001**, *105*, 9498–9508.
[22] K. Funatsu, T. Imamura, A. Ichimura, Y. Sasaki, *Inorg. Chem.* **1998**, *37*, 1798–1804.
[23] R. A. Jensen, R. F. Kelley, S. Joong Lee, M. R. Wasielewski, J. T. Hupp, D. M. Tiede, *Chem. Commun.* **2008**, 1886–1888.
[24] A. M. Shachter, E. B. Fleischer, R. C. Haltiwanger, *J. Chem. Soc. Chem. Commun.* **1988**, 960–961.
[25] R. F. Kelley, R. H. Goldsmith, M. R. Wasielewski, *J. Am. Chem. Soc.* **2007**, *129*, 6384–6385.
[26] Y. Shinozaki, K. Ohkubo, S. Fukuzumi, K. Sugawa, J. Otsuki, *Chem. Eur. J.* **2016**, *22*, 1165–1176.
[27] Y. Shinozaki, T. Tsubomura, K. Sugawa, J. Otsuki, *Tetrahedron Lett.* **2016**, *57*, 48–52.
[28] Y. Shinozaki, G. Richards, K. Ogawa, A. Yamano, K. Ohara, K. Yamaguchi, S.-i. Kawano, K. Tanaka, Y. Araki, T. Wada, J. Otsuki, *J. Am. Chem. Soc.* **2013**, *135*, 5262–5265.
[29] A. Tsuda, S. Sakamoto, K. Yamaguchi, T. Aida, *J. Am. Chem. Soc.* **2003**, *125*, 15722–15723.
[30] V. L. Gunderson, M. R. Wasielewski, *Chem. Phys. Lett.* **2013**, *556*, 303–307.
[31] R. Takahashi, Y. Kobuke, *J. Am. Chem. Soc.* **2003**, *125*, 2372–2373.
[32] M. Z. Papiz, S. M. Prince, T. Howard, R. J. Cogdell, N. W. Isaacs, *J. Mol. Biol.* **2003**, *326*, 1523–1538.
[33] A. W. Roszak, T. D. Howard, J. Southall, A. T. Gardiner, C. J. Law, N. W. Isaacs, R. J. Cogdell, *Science* **2003**, *302*, 1969–1972.
[34] S. Niwa, L.-J. Yu, K. Takeda, Y. Hirano, T. Kawakami, Z.-Y. Wang-Otomo, K. Miki, *Nature* **2014**, *508*, 228–232.
[35] A. D. Adler, F. R. Longo, J. D. Finarelli, J. Goldmacher, J. Assour, L. Korsakoff, *J. Org. Chem.* **1967**, *32*, 476.
[36] S. V. Bhosale, S. Hackbarth, S. J. Langford, S. V. Bhosale, *Chem. Asian J.* **2012**, *7*, 176–182.
[37] D. Sirbu, C. Turta, A. C. Benniston, F. Abou-Chahine, H. Lemmetyinen, N. V. Tkachenko, C. Wood, E. Gibson, *RSC Adv.* **2014**, *4*, 22733–22742.
[38] D.-F. Shi, R. T. Wheelhouse, D. Sun, L. H. Hurley, *J. Med. Chem.* **2001**, *44*, 4509–4523.
[39] R. S. Loewe, A. Ambroise, K. Muthukumaran, K. Padmaja, A. B. Lysenko, G. Mathur, Q. Li, D. F. Bocian, V. Misra, J. S. Lindsey, *J. Org. Chem.* **2004**, *69*, 1453–1460.
[40] Y. Zhou, K. T. Ngo, B. Zhang, Y. Feng, J. Rochford, *Organometallics* **2014**, *33*, 7078–7090.
[41] B. J. Littler, Y. Ciringh, J. S. Lindsey, *J. Org. Chem.* **1999**, *64*, 2864–2872.
[42] V. V. Krishnan, *J. Magn. Reson.* **1997**, *124*, 468–473.
[43] C. S. J. Jr., *Prog. Nucl. Magn. Reson. Spectrosc.* **1999**, *34*, 203–256.
[44] Y. Cohen, L. Avram, L. Frish, *Angew. Chem. Int. Ed.* **2005**, *44*, 520–554.
[45] R. Evans, Z. Deng, A. K. Rogerson, A. S. McLachlan, J. J. Richards, M. Nilsson, G. A. Morris, *Angew. Chem. Int. Ed.* **2013**, *52*, 3199–3202.
[46] E. B. Fleischer, C. K. Miller, L. E. Webb, *J. Am. Chem. Soc.* **1964**, *86*, 2342–2347.
[47] R. J. Abraham, G. R. Bedford, D. McNeillie, B. Wright, *Org. Magn. Reson.* **1980**, *14*, 418–425.
[48] P. S. Sobolev, V. P. Andreev, T. A. Ekimova, *Russ. J. Gen. Chem.* **2014**, *84*, 1399–1403.
[49] V. P. Andreev, P. S. Sobolev, N. S. Lebedeva, V. A. Tafeenko, *Russ. J. Gen. Chem.* **2015**, *85*, 906–910.
[50] V. P. Andreev, P. S. Sobolev, D. O. Zaitsev, S. M. Timofeeva, *Russ. J. Gen. Chem.* **2018**, *88*, 2108–2113.
[51] J. Rochford, A. D. Rooney, M. T. Pryce, *Inorg. Chem.* **2007**, *46*, 7247–7249.
[52] M. Kubo, Y. Mori, M. Otani, M. Murakami, Y. Ishibashi, M. Yasuda, K. Hosomizu, H. Miyasaka, H. Imahori, S. Nakashima, *J. Phys. Chem. A* **2007**, *111*, 5136–5143.
[53] M. K. Chahal, H. B. Gobeze, W. A. Webre, P. A. Karr, D. T. Payne, K. Ariga, F. D'Souza, J. P. Hill, *Phys. Chem. Chem. Phys.* **2020**, *22*, 14356–14363.
[54] Y. Kuramochi, Y. Fujisawa, A. Satake, *J. Am. Chem. Soc.* **2020**, *142*, 705–709.
[55] J. Fujimoto, S. Hayashi, H. Kainuma, K. Manseki, T. Udagawa, H. Miyaji, *Chem. Asian J.* **2019**, *14*, 2567–2572.
[56] R. J. Abraham, S. C. M. Fell, K. M. Smith, *Org. Magn. Reson.* **1977**, *9*, 367–373.
[57] R. J. Abraham, C. J. Medforth, *Magn. Reson. Chem.* **1988**, *26*, 803–812.
[58] Y. Shinozaki, Y. Mizumura, Y. Kida, K. Sugawa, K. Wada, S. Kishiro, J. Otsuki, *Chem. Lett.* **2016**, *45*, 1123–1125.
[59] J. J. P. Stewart, *J. Mol. Model.* **2007**, *13*, 1173–1213.
[60] C. Stangel, F. Plass, A. Charisiadis, E. Giannoudis, G. Chararalambidis, K. Karikis, G. Rotas, G. E. Zervaki, N. N. Lathiotakis, N. Tagmatarchis, A. Kahnt, A. G. Coutsolelos, *Phys. Chem. Chem. Phys.* **2018**, *20*, 21269–21279.
[61] P. Klán, J. Wirz, *Photochemistry of Organic Compounds*, (Eds.: Wiley, **2009**.
[62] G. L. Closs, L. E. Closs, *J. Am. Chem. Soc.* **1963**, *85*, 818–819.
[63] W. Delong, W. Lanying, W. Yongling, S. Shuang, F. Juntao, Z. Xing, *Eur. J. Med. Chem.* **2017**, *130*, 286–307.
[64] Q. Liu, C. Li, E. Jin, Z. Lu, Y. Chen, F. Li, Z. Bo, *ACS Appl. Mater. Interf.* **2014**, *6*, 1601-1607.
[65] Y. Kubo, M. Ando, H. Tanaka, S. Osaka, T. Matsumoto, H. Nakata, D. Terada, T. Nitabaru, (Fujifilm), WO2015030057A1, **2015**.
[66] H. Takezawa, M. Hayashi, Y. Iwasawa, M. Hosoi, Y. Iida, Y. Tsuchiya, M. Horie, T. Kamei, (Banyu Pharmaceutical), WO9005132A1, **1990**.
[67] C. Kremoser, U. Abel, C. Steeneck, O. Kinzel, (Phenex Pharmaceuticals), WO2011020615A1, **2010**.
[68] R. Takahashi, Y. Kobuke, *J. Org. Chem.* **2005**, *70*, 2745–2753.

10.1002/chem.202003327

Entry for the Table of Contents

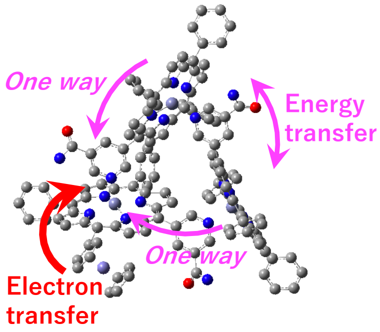

Zinc *meso*-(*meta*-pyridyl)porphyrin forms a trimer in solution over wide temperature and concentration ranges. A supramolecular light-harvesting/charge separation system, a rare example in which energy gradient is incorporated and reductive quenching is involved, was constructed using this motif of self-assembly.